PERGAMON

Chemical Engineering Science 58 (2003) 4449–4464

Chemical Engineering Science

www.elsevier.com/locate/ces

Boundary effects on osmophoresis: motion of a spherical vesicle parallel to two plane walls

Po Y. Chen, Huan J. Keh*

Department of Chemical Engineering, National Taiwan University, Taipei 106-17, Taiwan, ROC

Received 16 January 2003; received in revised form 7 July 2003; accepted 9 July 2003

Abstract

A theoretical study is presented for the quasisteady osmophoretic motion of a spherical vesicle in a solution located between two infinite parallel plane walls in the limit of negligible Reynolds and Peclet numbers. The applied solute concentration gradient is uniform and parallel to the two plane walls, which may be either impermeable to the solute molecules or prescribed with the far-field concentration distribution. The presence of the neighboring walls causes two basic effects on the vesicle velocity: first, the local concentrations on both sides of the vesicle surface are altered by the walls, thereby speeding up or slowing down the vesicle; secondly, the walls enhance the viscous interaction effect on the moving vesicle. To solve the equations of conservation of mass and momentum, the general solutions are constructed from the fundamental solutions in both the rectangular and the spherical coordinate systems. The boundary conditions are enforced first at the plane walls by the Fourier transforms and then on the vesicle surface by a collocation technique. Numerical results for the osmophoretic velocity of the vesicle relative to that under identical conditions in an unbounded solution are presented for various values of the relevant properties of the vesicle as well as the relative separation distances between the vesicle and the two plates. For the special case of osmophoretic motions of a spherical vesicle parallel to a single plate and on the central plane of a slit, the collocation results agree well with the approximate analytical solutions obtained by using a method of reflections. The presence of the lateral walls can reduce or enhance the vesicle velocity, depending upon the relevant properties of the vesicle, the relative vesicle-wall separation distances, and the solutal boundary condition at the walls. In general, the boundary effect on osmophoresis is quite complicated in comparison with that on sedimentation.

Keywords: Osmophoresis; Colloidal phenomena; Fluid Mechanics; Semipermeable vesicle; Boundary effect; Plane walls

1. Introduction

The existence of a solute concentration gradient in an unbounded solvent does not by itself generate an appreciable volume flow. However, when two solutions differing in concentration are separated by a semipermeable membrane, i.e., a membrane that permits the passage of solvent but not solute, it is observed that the solvent at the side of lower concentration tends to pass through the membrane into the solution of higher concentration, and thereby dilute it. This phenomenon is called osmosis; it still occurs to a certain extent when the solute molecules can cross the membrane but experience more resistance in doing so than the solvent molecules. The osmotic flow of solvent can be prevented by applying a pressure to the solution of higher concentration which is greater than the pressure on the solution at the other side by an amount equal to $\sigma\Delta\Pi$, where $\Delta\Pi$ is the difference in osmotic pressure between the two solutions and σ is a reflection coefficient characterizing the degree to which the solute molecules are rejected from the membrane. For a semipermeable membrane, $\sigma = 1$; for a non-selective membrane, $\sigma = 0$. For an ideal solution (with very low solute concentration), the osmotic pressure Π is linearly related to the solute concentration C by the van't Hoff law, $\Pi = CRT$, where R is the gas constant and T is the absolute temperature.

A vesicle is a body of fluid bounded by a thin, rigid, semipermeable membrane which responds to the variations of osmotic pressure in the surrounding fluid. When the vesicle is placed in a solution possessing a solute concentration

* Corresponding author. Tel.: +886-223-6354-62; fax: +886-2-23623040.
E-mail address: huan@ntu.edu.tw (H. J. Keh).

0009-2509/$ - see front matter © 2003 Elsevier Ltd. All rights reserved.
doi:10.1016/S0009-2509(03)00342-7

gradient, one pole of the vesicle sees a higher solute concentration (and hence a higher osmotic pressure) than the opposite pole. The osmotic driving force causes solvent to cross the vesicle's membrane from inside to outside at the high concentration end, and from outside to inside at the low concentration end. The vesicle thus functions as a microengine sucking in fluid on one side and ejecting fluid on the other, thereby advancing toward regions of low concentration. This movement of vesicle is termed osmophoresis (Gordeon, 1981; Anderson, 1983, 1986), which could be a transport mechanism for vesicles within cells, and this phenomenon could play some role in the motility of vesicles and cells. Applications of osmophoretic motion might also be found in the targeting of encapsulated drugs and other agents toward a microscopic region.

The osmophoretic motion of a spherical vesicle with a very thin membrane in an unbounded fluid with a prescribed linear solute concentration distribution $C_\infty(\mathbf{x})$ has been theoretically investigated by Anderson (1983) for a quite general case. In most physically realistic systems, the velocity $\mathbf{U}_0$ of a semipermeable vesicle of radius a is related to the uniform concentration gradient ∇C_∞ by the expression

$$\mathbf{U}_0 = -A\nabla C_\infty, \tag{1a}$$

where the vesicle's mobility

$$A = aL_pRT(2 + 2\bar{\kappa} + \kappa)^{-1} \tag{1b}$$

with dimensionless parameters

$$\kappa = aL_pRTC_0/D, \tag{2a}$$

$$\bar{\kappa} = aL_pRT\bar{C}/\bar{D}. \tag{2b}$$

In the above equations, L_p is the hydraulic coefficient which is a constant for a given membrane and solvent, $\bar{D}$ and D are the solute diffusion coefficients inside and outside the vesicle, respectively, $\bar{C}$ is the average internal concentration of solute, and C_0 denotes the value of C_∞ at the position of the vesicle center. The van't Hoff law was used in the derivation of Eq. (1); if Π is not a linear function of C at fixed temperature, then RT must be replaced by $\partial\Pi/\partial C$, evaluated at C_0 in Eqs. (1b) and (2a) and at $\bar{C}$ in Eq. (2b). Typical values in aqueous solutions for the parameters in Eq. (1) are $L_p = 10^{-9}$ m^2 s/kg, $|\nabla C_\infty| = 10^5$ mol/m^4 and κ (or $\bar{\kappa}$) $= 2.5$. Eq. (1) shows that the vesicle always moves toward regions of lower C_∞, no matter what the relative values of C_0 and $\bar{C}$ are. Increases in the value of parameter κ or $\bar{\kappa}$ have a retarding effect on the vesicle velocity. A recent experimental work reported that model lipid vesicles of a 10 μm radius in a sucrose concentration gradient of 10^4 mol/m^4 have a drift velocity of the order of a few micrometers per second (Nardi, Bruinsma, & Sackmann, 1999).

In practical applications of osmophoresis, vesicles are not isolated and will move in the presence of neighboring boundaries. Using a method of reflections, Anderson (1986) obtained analytically the migration velocity of a spherical vesicle undergoing osmophoresis along the axis of a long circular pore for the special case of $\kappa = \bar{\kappa} = 0$. His result indicates that the vesicle velocity *increases* monotonically as the ratio of vesicle-to-pore radii increases. This behavior, which is opposite to intuition and occurs because the flow of solvent accompanying the osmophoretic vesicle is opposite to the direction of vesicle movement, was also observed experimentally by Berg and Turner (1990). On the other hand, the osmophoretic motion of a spherical vesicle in an arbitrary direction with respect to a plane wall was examined by Keh and Yang (1993a,b) through an exact representation in spherical bipolar coordinates. Numerical results of wall-correction to Eq. (1) for the vesicle velocity were presented for various values of the relative separation distance and parameters κ and $\bar{\kappa}$. For the cases considered in this work, the osmophoretic mobility of the vesicle was also found to increase as the vesicle approaches the plane wall.

The objective of this article is to obtain exact numerical solutions and approximate analytical solutions for the osmophoretic motions of a spherical vesicle parallel to a single plane wall and to two plane walls at an arbitrary position between them. The plane walls may be either impermeable to the solute species or prescribed with the linear far-field solute concentration distribution. The effects of fluid inertia as well as solute convection are neglected. As it will be shown from the method-of-reflection analysis in Appendix A, for the case of a vesicle with $\kappa \gg 1+\bar{\kappa}$ undergoing osmophoresis near impermeable plane walls or of a vesicle with $\kappa \ll 1+\bar{\kappa}$ undergoing osmophoresis near plane walls prescribed with the far-field concentration distribution, the solute diffusion around the vesicle will generate smaller concentration gradients along the vesicle surface relative to those in an infinite medium. These concentration gradients reduce the osmophoretic velocity, although their action will be enhanced by the viscous interaction of the migrating vesicle with the walls. Both effects of this solutal retardation and the hydrodynamic enhancement increase as the ratios of the radius of the vesicle to its distances from the walls increase. Determining which effect is overriding at small vesicle-wall gap widths is a main target of this study.

2. Analysis

The quasisteady osmophoresis of a spherical vesicle of radius a surrounded by a thin semipermeable membrane in a fluid solution parallel to two infinite plane walls whose distances from the center of the vesicle are b and c, as shown in Fig. 1, is considered. Here (x, y, z), (ρ, ϕ, z), and (r, θ, ϕ) denote the rectangular, circular cylindrical, and spherical coordinate systems, respectively, and the origin of coordinates is chosen at the vesicle center. A linear concentration field $C_\infty(\mathbf{x})$ with a uniform solute gradient $-E_\infty\mathbf{e}_x$ $(=\nabla C_\infty$, where E_∞ is taken to be positive) is imposed in the ambient fluid far away from the vesicle, where $\mathbf{e}_x$ together with $\mathbf{e}_y$

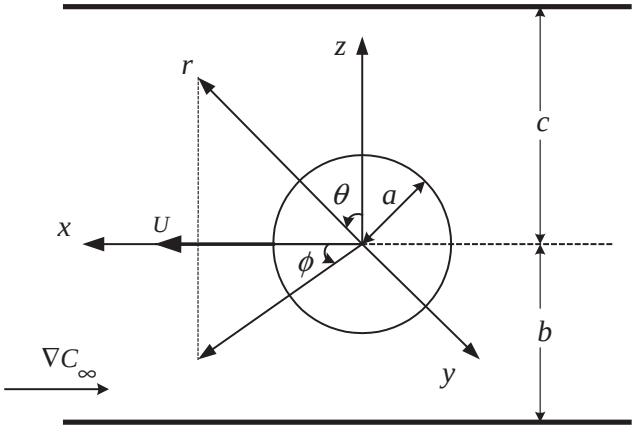

Fig. 1. Geometrical sketch for the osmophoresis of a spherical vesicle parallel to two plane walls at an arbitrary position between them.

and $\mathbf{e}_z$ are the unit vectors in rectangular coordinates. The vesicle is assumed to maintain its spherical shape and no solute can be transferred across its membrane. The objective is to determine the correction to Eq. (1) for the vesicle velocity due to the presence of the plane walls.

Before determining the osmophoretic velocity of the vesicle, the velocity field in the external fluid phase needs to be found. Because the boundary condition for the fluid velocity is coupled with the solute concentration field at the vesicle surface, it is necessary to determine the concentration distribution first.

2.1. Solute concentration distribution

The Peclet number of the steady system is assumed to be small. Hence, the conservation equation governing the solute concentration distribution $C(\mathbf{x})$ for the external fluid of constant solute diffusion coefficient D is the Laplace equation,

$$\nabla^2 C = 0 \quad (r \geqslant a). \tag{3a}$$

For the concentration filed $C_1(\mathbf{x})$ inside the vesicle, one has

$$\nabla^2 C_1 = 0 \quad (r \leqslant a). \tag{3b}$$

Since the radius of the vesicle is much greater than the thickness of its membrane, $r = a$ can represent both the inner and outer membrane surfaces of the vesicle. Thus, the concentration distribution is subject to the boundary conditions (Anderson, 1983; Keh & Yang, 1993a)

$$r = a: \quad \frac{\partial C_1}{\partial r} = \frac{\bar{\kappa}}{a}[C - C_0 - (C_1 - \bar{C})], \tag{4a}$$

$$\frac{\partial C}{\partial r} = \frac{\kappa}{a}[C - C_0 - (C_1 - \bar{C})], \tag{4b}$$

where the definition of the parameters κ and $\bar{\kappa}$ (proportional to C_0 and $\bar{C}$, respectively) is given by Eq. (2).

The solute concentration far away from the vesicle approaches the undisturbed values. We can write

$$z = c, -b: \quad \frac{\partial C}{\partial z} = 0, \tag{5}$$

$$\rho \to \infty: \quad C \to C_\infty = C_0 - E_\infty x. \tag{6}$$

Note that the boundary conditions given by Eq. (5) apply for the case of two impermeable plane walls. For the case of osmophoretic motion of a vesicle parallel to two plane walls prescribed with a linear concentration profile consistent with the far-field solute distribution, Eq. (5) should be replaced by

$$z = c, -b: \quad C = C_\infty. \tag{7}$$

Since the governing equations and boundary conditions are linear, one can express the external concentration distribution C, which is symmetric with respect to y and antisymmetric with respect to x, as the superposition

$$C = C_w + C_p. \tag{8}$$

Here, C_w is a double Fourier integral solution of Eq. (3a) in rectangular coordinates that represents the disturbance produced by the plane walls plus the undisturbed concentration field and is given by

$$C_w = C_0 - E_\infty x - E_\infty \int_0^\infty \int_0^\infty (X e^{\gamma z} + Y e^{-\gamma z}) \sin(\alpha x)\cos(\beta y)\, d\alpha\, d\beta, \tag{9}$$

where X and Y are unknown functions of separation variables α and β, and $\gamma = (\alpha^2 + \beta^2)^{1/2}$. The second term on the right-hand side of Eq. (8), C_p, is a solution of Eq. (3a) in spherical coordinates representing the disturbance generated by the vesicle and is given by an infinite series in harmonics,

$$C_p = -E_\infty \sum_{n=1}^{\infty} R_n r^{-n-1} P_n^1(\mu)\cos\phi, \tag{10}$$

where P_n^1 is the associated Legendre function of order n and degree one, μ is used to denote $\cos\theta$ for brevity, and R_n are unknown constants. Note that a solution for C of the form given by Eqs. (8)–(10) immediately satisfies the boundary condition at infinity in Eq. (6). Since the solute concentration is finite for any position in the interior of the vesicle, the solution to Eq. (3b) can be written as

$$C_1 = \bar{C} - E_\infty x - E_\infty \sum_{n=1}^{\infty} \bar{R}_n r^n P_n^1(\mu)\cos\phi, \tag{11}$$

where $\bar{R}_n$ are unknown constants.

Substituting the concentration distribution C given by Eqs. (8)–(10) into the boundary conditions in Eq. (5) or (7) and applying the Fourier sine and cosine transforms on the variables x and y, respectively, lead to a solution for the functions X and Y in terms of the coefficients R_n. After the

substitution of this solution into Eq. (9) and utilization of the integral representations of the modified Bessel functions of the second kind, the concentration distribution C can be expressed as

$$C = C_0 - E_\infty x - E_\infty \sum_{n=1}^{\infty} R_n \delta_n^{(1)}(r,\mu)\cos\phi, \tag{12}$$

where the function $\delta_n^{(1)}(r,\mu)$ is defined by Eq. (B.1) in Appendix B. Applying the boundary conditions given by Eq. (4) to Eqs. (11) and (12) yields

$$\sum_{n=1}^{\infty} [R_n \bar{\kappa}\delta_n^{(1)}(a,\mu) - \bar{R}_n(\bar{\kappa}+n)a^n P_n^1(\mu)] = a(1-\mu^2)^{1/2}, \tag{13a}$$

$$\sum_{n=1}^{\infty} \{R_n[\kappa\delta_n^{(1)}(a,\mu) - a\delta_n^{(2)}(a,\mu)] - \bar{R}_n \kappa a^n P_n^1(\mu)\} = a(1-\mu^2)^{1/2}, \tag{13b}$$

where the definition of the function $\delta_n^{(2)}(r,\mu)$ is given by Eq. (B.2). Note that the dependence on ϕ factors out in Eq. (13) and the definite integrals in $\delta_n^{(1)}$ and $\delta_n^{(2)}$ must be performed numerically.

To satisfy the conditions in Eq. (13) exactly along the entire surface of the vesicle would require the solution of the entire infinite array of unknown constants R_n and $\bar{R}_n$. However, the collocation method (O'Brien, 1968; Ganatos, Weinbaum, & Pfeffer, 1980) enforces the boundary conditions at a finite number of discrete points on the half-circular generating arc of the sphere (from $\theta = 0$ to π) and truncates the infinite series in Eqs. (11) and (12) into finite ones. If the spherical boundary is approximated by satisfying the conditions of Eq. (4) at M discrete points on its generating arc, the infinite series in Eqs. (11) and (12) are truncated after M terms, resulting in a system of $2M$ simultaneous linear algebraic equations in the truncated form of Eq. (13). This matrix equation can be numerically solved to yield the $2M$ unknown constants R_n and $\bar{R}_n$ required in the truncated form of Eqs. (11) and (12) for the solute concentration distribution. The accuracy of the boundary-collocation/truncation technique can be improved to any degree by taking a sufficiently large value of M. Naturally, as $M \to \infty$ the truncation error vanishes and the overall accuracy of the solution depends only on the numerical integration required in evaluating the matrix elements.

2.2. Fluid velocity distribution

With knowledge of the solution for the solute concentration distribution on the vesicle surface which drives the osmophoretic migration, we can now proceed to find the flow field. The fluid is assumed to be incompressible and Newtonian. Owing to the low Reynolds number, the fluid motion outside the vesicle is governed by the Stokes equations,

$$\eta\nabla^2\mathbf{v} - \nabla p = \mathbf{0}, \tag{14a}$$

$$\nabla\cdot\mathbf{v} = 0, \tag{14b}$$

where $\mathbf{v}(\mathbf{x})$ is the velocity field for the external flow, $p(\mathbf{x})$ is the corresponding dynamic pressure distribution, and η is the fluid viscosity.

The boundary conditions for the fluid velocity at the vesicle surface (Anderson, 1983; Keh & Yang, 1993b), on the plane walls, and far removed from the vesicle are

$$r = a: \quad \mathbf{v} = \mathbf{U} + a\boldsymbol{\Omega}\times\mathbf{e}_r + L_p RT[C - C_0 - (C_1 - \bar{C})]\mathbf{e}_r, \tag{15}$$

$$z = c, -b: \quad \mathbf{v} = \mathbf{0}, \tag{16}$$

$$\rho \to \infty: \quad \mathbf{v} = \mathbf{0}. \tag{17}$$

Here, $\mathbf{e}_r$ together with $\mathbf{e}_\theta$ and $\mathbf{e}_\phi$ are the unit vectors in spherical coordinates, and $\mathbf{U} = U\mathbf{e}_x$ and $\boldsymbol{\Omega} = \Omega\mathbf{e}_y$ are the translational and angular velocities of the vesicle undergoing osmophoresis to be determined. For the asymmetric problem as $b \neq c$, the assumption that the sphere would migrate in a direction parallel to the concentration gradient is justified in the absence of inertia.

A fundamental solution to Eq. (14) which satisfies Eqs. (16) and (17) is

$$\mathbf{v} = v_x\mathbf{e}_x + v_y\mathbf{e}_y + v_z\mathbf{e}_z, \tag{18}$$

where

$$v_x = \sum_{n=1}^{\infty}[A_n(A_n' + \alpha_n') + B_n(B_n' + \beta_n') + C_n(C_n' + \gamma_n')], \tag{19a}$$

$$v_y = \sum_{n=1}^{\infty}[A_n(A_n'' + \alpha_n'') + B_n(B_n'' + \beta_n'') + C_n(C_n'' + \gamma_n'')], \tag{19b}$$

$$v_z = \sum_{n=1}^{\infty}[A_n(A_n''' + \alpha_n''') + B_n(B_n''' + \beta_n''') + C_n(C_n''' + \gamma_n''')]. \tag{19c}$$

Here, the primed A_n, B_n, C_n, α_n, β_n, and γ_n are functions of position involving associated Legendre functions of μ or $\cos\theta$ defined by Eq. (2.6) and in the form of integration (which must be performed numerically) defined by Eq. (C1) of Ganatos et al. (1980), and A_n, B_n, and C_n are unknown constants.

The boundary condition that remains to be satisfied is that on the vesicle surface. Substituting Eqs. (12) and (18) into

Eq. (15), one obtains

$$\sum_{n=1}^{\infty}[A_n(A_n'+\alpha_n')+B_n(B_n'+\beta_n')+C_n(C_n'+\gamma_n')]$$
$$=U+a\Omega\mu-L_pRTE_\infty\sum_{n=1}^{\infty}[R_n\delta_n^{(1)}(a,\mu)-\bar{R}_n a^n P_n^1(\mu)](1-\mu^2)^{1/2}\cos^2\phi, \quad (20a)$$

$$\sum_{n=1}^{\infty}[A_n(A_n''+\alpha_n'')+B_n(B_n''+\beta_n'')+C_n(C_n''+\gamma_n'')]$$
$$=-L_pRTE_\infty\sum_{n=1}^{\infty}[R_n\delta_n^{(1)}(a,\mu)-\bar{R}_n a^n P_n^1(\mu)](1-\mu^2)^{1/2}\sin\phi\cos\phi, \quad (20b)$$

$$\sum_{n=1}^{\infty}[A_n(A_n'''+\alpha_n''')+B_n(B_n'''+\beta_n''')+C_n(C_n'''+\gamma_n''')]$$
$$=-a\Omega(1-\mu^2)^{1/2}\cos\phi-L_pRTE_\infty\sum_{n=1}^{\infty}[R_n\delta_n^{(1)}(a,\mu)-\bar{R}_n a^n P_n^1(\mu)]\mu\cos\phi. \quad (20c)$$

The first $2M$ coefficients R_n and $\bar{R}_n$ have been determined through the procedure given in the previous subsection.

Careful examination of Eq. (20) shows that the solution of the coefficient matrix generated is independent of the ϕ coordinate of the boundary points on the surface of the sphere $r=a$. Thus, these relations can be satisfied by utilizing the collocation technique presented for the solution of the solute concentration field. At the vesicle surface, Eq. (20) is applied at N discrete points (values of θ between 0 and π) and the infinite series in Eq. (19) are truncated after N terms. This generates a set of $3N$ linear algebraic equations for the $3N$ unknown coefficients A_n, B_n, and C_n. The fluid velocity field outside the vesicle is completely obtained once these coefficients are solved for a sufficiently large value of N.

2.3. Derivation of the vesicle velocities

The drag force and torque exerted by the external fluid on the spherical vesicle can be determined from (Ganatos et al., 1980)

$$\mathbf{F}=-8\pi\eta A_1\mathbf{e}_x, \quad (21a)$$

$$\mathbf{T}=-8\pi\eta C_1\mathbf{e}_y. \quad (21b)$$

These expressions show that only the lowest-order coefficients A_1 and C_1 contribute to the hydrodynamic force and couple acting on the vesicle.

Because the vesicle is freely suspended in the surrounding fluid, the net force and torque exerted on the vesicle must vanish. Applying this constraint to Eq. (21), one has

$$A_1=C_1=0. \quad (22)$$

To determine the translational and angular velocities U and Ω of the vesicle, Eq. (22) and the $3N$ algebraic equations resulting from Eq. (20) are to be solved simultaneously.

When the translational and rotational velocities in Eq. (15) are disabled (i.e., $\mathbf{U}=\mathbf{0}$ and $\mathbf{\Omega}=\mathbf{0}$ are set), the force and torque obtained from Eq. (21) can be taken as the osmophoretic force and torque exerted on the vesicle near the walls due to the solute concentration gradient ∇C_∞. This force and torque can be expressed as

$$\mathbf{F}=6\pi\eta a\mathbf{U}_0F^*, \quad (23a)$$

$$\mathbf{T}=8\pi\eta a^2\mathbf{e}_z\times\mathbf{U}_0T^*, \quad (23b)$$

where F^* and T^* are the normalized magnitudes of the osmophoretic force and torque, respectively, and $\mathbf{U}_0$ is a characteristic velocity (the osmophoretic velocity of the vesicle in the solution in the absence of the boundary walls) given by Eq. (1).

3. Results and discussion

The solution for the osmophoretic motion of a spherical vesicle parallel to two plane walls at an arbitrary position between them, obtained by using the boundary collocation method described in the previous section, is presented in this section. The system of linear algebraic equations to be solved for the coefficients R_n and $\bar{R}_n$ is constructed from Eq. (13), while that for A_n, B_n, and C_n is composed of Eq. (20). All the numerical integrations to evaluate the primed α_n, β_n, and γ_n as well as $\delta_n^{(i)}$ functions were done by the 80-point Gauss–Laguerre quadrature.

When specifying the points along the semicircular generating arc of the spherical vesicle (with a constant value of ϕ) where the boundary conditions are to be exactly satisfied, the first points that should be chosen are $\theta=0$ and π, since these points define the projected area of the vesicle normal to the direction of motion and control the gaps between the vesicle and the neighboring plates. In addition, the point $\theta=\pi/2$ is also important. However, an examination of the systems of linear algebraic equations in Eqs. (13) and (20) shows that the matrix equations become singular if these points are used. To overcome this difficulty, these points are replaced by closely adjacent points, i.e., $\theta=\delta$, $\pi/2-\delta$, $\pi/2+\delta$, and $\pi-\delta$ (Ganatos et al., 1980). Additional points along the boundary are selected as mirror-image pairs about the plane $\theta=\pi/2$ to divide the two quarter-circular arcs of the vesicle into equal segments. The optimum value of δ in this work is found to be 0.1°, with which the numerical results of the vesicle velocities converge satisfactorily. In selecting the boundary points, any value of ϕ may be used except for $\phi=0,\pi/2$, and π since the matrix equation (20) is singular for these values.

Table 1
Numerical results of the normalized osmophoretic force F^* and torque T^* on a spherical vesicle near an impermeable plane wall (with $c \to \infty$) caused by a parallel solute concentration gradient for the case of $\kappa = \bar{\kappa} = 0$

a/b	F^*			T^*		
	$N = M = 30$	$N = M = 36$	$N = M = 42$	$N = M = 30$	$N = M = 36$	$N = M = 42$
0.2	1.12862	1.12862	1.12862	0.00047	0.00047	0.00047
0.4	1.30916	1.30916	1.30916	0.00807	0.00807	0.00807
0.6	1.59964	1.59964	1.59964	0.04905	0.04905	0.04905
0.8	2.20976	2.20976	2.20976	0.23722	0.23722	0.23722
0.9	2.99177	2.99177	2.99177	0.60603	0.60603	0.60603
0.95	3.9833	3.9834	3.9834	1.1827	1.1826	1.1826
0.99	7.3167	7.2881	7.2881	3.3824	3.4155	3.4155
0.995	9.014	8.927	8.927	4.431	4.550	4.550
0.999	11.74	11.36	11.36	5.628	6.153	6.153

3.1. Motion parallel to a single plane wall

In Table 1, a number of numerical solutions of the normalized osmophoretic force and torque acting on a spherical vesicle near an impermeable plane wall (with $c \to \infty$) caused by a parallel solute concentration gradient, defined by Eq. (23), are presented for various values of the spacing parameter a/b using the collocation technique for the case of $\kappa = \bar{\kappa} = 0$. All of these results were obtained by choosing the number of collocation points N $(=M)$ equal to 30, 36, and 42 to show their convergence. The rate of convergence is rapid for small values of a/b and deteriorates monotonically as the distance between the vesicle and the planar boundary decreases. Opposite to intuition, the results in Table 1 illustrate that the osmophoretic force exerted on the vesicle increases monotonically as the parameter a/b increases.

The collocation solutions for the translational and rotational velocities of a spherical vesicle undergoing osmophoresis parallel to a plane wall for different values of the parameters κ, $\bar{\kappa}$, and a/b are presented in Tables 2 and 3 for the cases of an impermeable wall and a wall with the imposed far-field solute concentration gradient, respectively. The velocity for the osmophoretic motion of an identical vesicle in an infinite fluid, U_0, given by Eq. (1), is used to normalize the boundary-corrected values. All of the results obtained under the collocation scheme converge satisfactorily to at least the significant figures shown in the tables. Again, the accuracy and convergence behavior of the truncation technique is principally a function of the ratio a/b. For the most difficult case with $a/b = 0.999$, the numbers of collocation points $M = 36$ and $N = 36$ are sufficiently large to achieve this convergence.

In Appendix A, an approximate analytical solution for the same osmophoretic motion as that considered here is also obtained by using a method of reflections. The translational and angular velocities of a spherical vesicle near a lateral plate is given by Eqs. (A.11a) and (A.11b), which are power series expansions in λ $(=a/b)$. The values of the wall-corrected normalized vesicle velocities calculated from this asymptotic solution, with the $O(\lambda^8)$ term neglected, are also listed in Tables 2 and 3 for comparison. It can be seen that the asymptotic formula of Eq. (A.11a) from the method of reflections for U/U_0 agrees very well with the exact results as long as $\lambda \leqslant 0.8$; the errors in all cases are less than 3.2%. However, the accuracy of Eqs. (A.11a) and (A.11b) [especially of Eq. (A.11b) for $a\Omega/U_0$, in which the leading term is $O(\lambda^4)$] deteriorates rapidly, as expected, when the relative spacing between the vesicle and the plane wall becomes small. It can be found that the collocation solutions for U/U_0 and $a\Omega/U_0$ obtained here are much more accurate than the corresponding numerical solutions obtained by using bispherical coordinates (Keh & Yang, 1993b) in comparison with the reflection results.

The exact numerical solutions for the normalized velocities U/U_0 and $a\Omega/U_0$ of a spherical vesicle undergoing osmophoresis parallel to a plane wall as functions of a/b are depicted in Figs. 2 and 3 for various values of κ and $\bar{\kappa}$. It can be seen that the wall-corrected normalized osmophoretic mobility U/U_0 of the vesicle decreases with an increase in κ and with a decrease in $\bar{\kappa}$ for the case of an impermeable wall (the boundary condition (5) is used), but increases with an increase in κ and with a decrease in $\bar{\kappa}$ for the case of a plane wall prescribed with the far-field solute concentration distribution (the boundary condition (7) is used), keeping each other parameter unchanged. This decrease and increase in the vesicle mobility becomes more pronounced as a/b increases. This behavior is expected knowing that the solute concentration gradients along the vesicle surface near an impermeable wall decrease as the ratio $\kappa/(1+\bar{\kappa})$ increases and these concentration gradients near a wall with the imposed far-field concentration gradient increase as $\kappa/(1+\bar{\kappa})$ increases (see the analysis in Appendix A). When $\kappa = 1+\bar{\kappa}$, the two types of plane wall will result in the same effects on the osmophoretic motion of the vesicle. In this particular case, the effect of solutal interaction between the vesicle and the wall disappears, and the relative osmophoretic mobility of the vesicle is independent of the value of either κ or $\bar{\kappa}$ and increases monotonically with a/b solely owing to the hydrodynamic enhancement exerted by the presence of the wall.

Table 2
Normalized translational and rotational velocities of a spherical vesicle undergoing osmophoresis parallel to a single impermeable plane wall computed from the exact boundary-collocation solution and the asymptotic method-of-reflection solution

a/b	U/U_0		$a\Omega/U_0$	
	Exact solution	Asymptotic solution	Exact solution	Asymptotic solution
$\kappa = \bar{\kappa} = 0$				
0.2	1.00245	1.00244	0.00060	0.00061
0.4	1.01905	1.01893	0.00998	0.01052
0.6	1.06651	1.06501	0.05604	0.06424
0.8	1.19518	1.17331	0.23161	0.27075
0.9	1.37549	1.27325	0.50444	0.51321
0.95	1.6066	1.34153	0.8468	0.69553
0.99	2.3358	1.40749	1.8148	0.88087
0.995	2.647		2.245	
0.999	3.049		2.838	
$\kappa = 10,\ \bar{\kappa} = 0$				
0.2	1.00118	1.00118	0.00060	0.00059
0.4	1.00839	1.00830	0.00976	0.00884
0.6	1.02411	1.02406	0.05141	0.03568
0.8	1.04507	1.05284	0.17650	0.05681
0.9	1.04477	1.07731	0.30197	0.02530
0.95	1.0203	1.09409	0.3877	−0.01687
0.99	0.9038	1.11055	0.4433	−0.06996
0.995	0.853		0.436	
0.999	0.783		0.431	
$\kappa = 0,\ \bar{\kappa} = 10$				
0.2	1.00245	1.00245	0.00060	0.00061
0.4	1.01921	1.01906	0.01002	0.01094
0.6	1.06883	1.06653	0.05698	0.07153
0.8	1.21930	1.18185	0.24760	0.32536
0.9	1.47298	1.29055	0.58685	0.63777
0.95	1.8744	1.36546	1.1032	0.87739
0.99	3.7155	1.43814	3.2605	1.12360
0.995	4.804		4.663	
0.999	6.458		7.126	

Examination of the results shown in Tables 2 and 3 and Figs. 2a and 3a reveals an interesting feature. For the case that the wall is an impermeable plane under the situation of $\kappa \gg 1 + \bar{\kappa}$, the osmophoretic mobility of the vesicle increases with an increase in a/b as a/b is small, but decreases from a maximum with increasing a/b as a/b is sufficiently large. When the gap between the vesicle and the wall turns thin, the vesicle can even move slower than it would at $a/b = 0$. For example, as $\kappa = 10$, $\bar{\kappa} = 0$ and $a/b = 0.999$, the osmophoretic velocity can be as much as 22% lower than the value with the wall being far away from the vesicle. Under the situations of $\kappa \leqslant 1 + \bar{\kappa}$, the osmophoretic mobility of the vesicle near the impermeable wall is a monotonically increasing function of a/b. For the case that a linear concentration profile is prescribed on the plane wall which is consistent with the far-field solute distribution under the situation of $\kappa \ll 1 + \bar{\kappa}$, the osmophoretic mobility of the vesicle first goes through a maximum with the increase of a/b from $a/b = 0$ and then decreases monotonically. Again, the value of U/U_0 can be less than unity when $a/b \to 1$. Under the situation of $\kappa \geqslant 1 + \bar{\kappa}$, the osmophoretic mobility of the vesicle near the wall prescribed with the far-field concentration distribution becomes a monotonically increasing function of a/b. This interesting feature that U/U_0 may not be a monotonic function of a/b and can even be smaller than unity is understandable because the wall effect of hydrodynamic enhancement on the vesicle is in the competition with the wall effect of solutal retardation when a vesicle with large value of $\kappa/(1 + \bar{\kappa})$ is undergoing osmophoretic motion parallel to an impermeable plate or when a vesicle with small value of $\kappa/(1 + \bar{\kappa})$ is moving near a lateral plate with the imposed far-field concentration gradient. A careful examination of the asymptotic formula for U/U_0 given by Eq. (A.11a) shows a good agreement of the numerical outcome in Figs. 2a and 3a with the analytical solution.

Table 3
Normalized translational and rotational velocities of a spherical vesicle undergoing osmophoresis parallel to a single plane wall prescribed with the far-field solute concentration profile computed from the exact boundary-collocation solution and the asymptotic method-of-reflection solution

a/b	U/U_0		$a\Omega/U_0$	
	Exact solution	Asymptotic solution	Exact solution	Asymptotic solution
$\kappa=\bar{\kappa}=0$				
0.2	1.00144	1.00144	0.00060	0.00060
0.4	1.01059	1.01048	0.00982	0.00941
0.6	1.03357	1.03291	0.05280	0.04543
0.8	1.08412	1.08064	0.19413	0.12984
0.9	1.14050	1.12400	0.36882	0.19186
0.95	1.1987	1.15396	0.5393	0.22633
0.99	1.3237	1.18323	0.8565	0.25464
0.995	1.357		0.952	
0.999	1.382		1.068	
$\kappa=10,\ \bar{\kappa}=0$				
0.2	1.00270	1.00270	0.00060	0.00061
0.4	1.02130	1.02115	0.01004	0.01109
0.6	1.07668	1.07431	0.05753	0.07399
0.8	1.24246	1.20367	0.25303	0.34378
0.9	1.50675	1.32514	0.59729	0.67978
0.95	1.8786	1.40858	1.0821	0.93873
0.99	3.0347	1.48937	2.5159	1.20547
0.995	3.479		3.118	
0.999	3.973		3.899	
$\kappa=0,\ \bar{\kappa}=10$				
0.2	1.00144	1.00143	0.00060	0.00060
0.4	1.01044	1.01035	0.00979	0.00899
0.6	1.03136	1.03139	0.05191	0.03814
0.8	1.06415	1.07211	0.18097	0.07523
0.9	1.07677	1.10670	0.31581	0.06730
0.95	1.0690	1.13003	0.4184	0.04447
0.99	1.0131	1.15258	0.5419	0.01191
0.995	0.987		0.567	
0.999	0.947		0.605	

The results in Tables 2 and 3 and Figs. 2b and 3b indicate that the spherical vesicle undergoing osmophoresis parallel to a plane wall rotates in the same direction as that for a rigid sphere migrating parallel to the wall but under a body-force field (e.g., a gravitational field). However, it is understood that the wall effect is always to reduce the migration velocity of the body-force-driven particle. For fixed values of κ and $\bar{\kappa}$, the magnitude of the normalized rotational velocity of the osmophoretic sphere near a plane wall is in general an increasing function of a/b. Analogous to the tendency of U/U_0, for a specified value of a/b, the magnitude of $a\Omega/U_0$ decreases with an increase in κ and with a decrease in $\bar{\kappa}$ for the osmophoresis of a vesicle parallel to an impermeable plate but increases with an increase in κ and with a decrease in $\bar{\kappa}$ for the migration parallel to a wall prescribed with the far-field concentration profile.

3.2. Motion parallel to two plane walls

In Table 4, numerical results of the normalized osmophoretic force and torque exerted on a spherical vesicle located between two parallel impermeable plane walls whose distance to one wall is three times as great as to the other wall (with $c=3b$) caused by a parallel solute concentration gradient are presented for various values of the parameter a/b using the collocation technique for the case of $\kappa=\bar{\kappa}=0$. Same as the results for a single plane wall given in Table 1, the results in Table 4 were obtained by choosing the number of collocation points N $(=M)$ equal to 30, 36, and 42 to show their convergence. Again, these results indicate that the osmophoretic force and torque acting on the vesicle are monotonic increasing function of a/b.

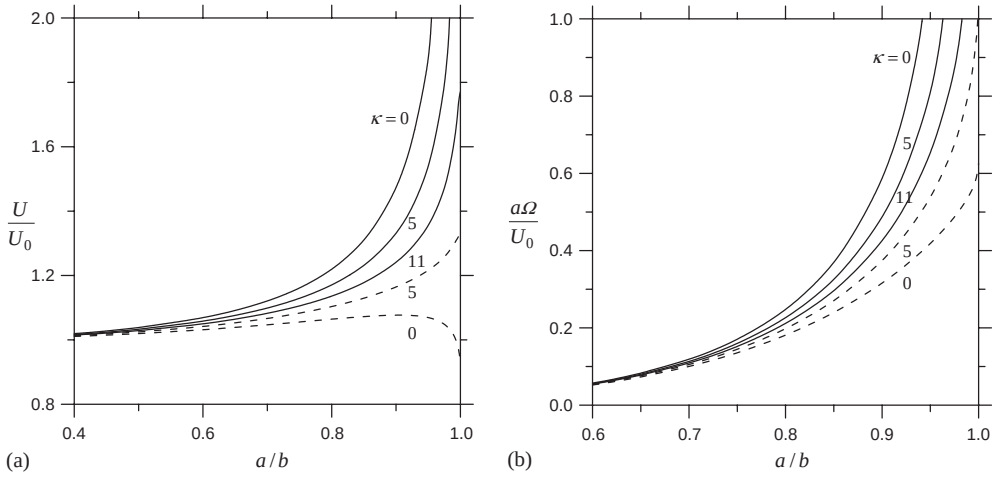

Fig. 2. Plots of the normalized velocities of a spherical vesicle with $\bar{\kappa} = 10$ undergoing osmophoresis parallel to a plane wall versus the separation parameter a/b for various values of κ: (a) translational velocity U/U_0; (b) rotational velocity $a\Omega/U_0$. The solid curves represent the case of an impermeable wall, and the dashed curves denote the case of a wall on which the far-field solute concentration gradient is imposed.

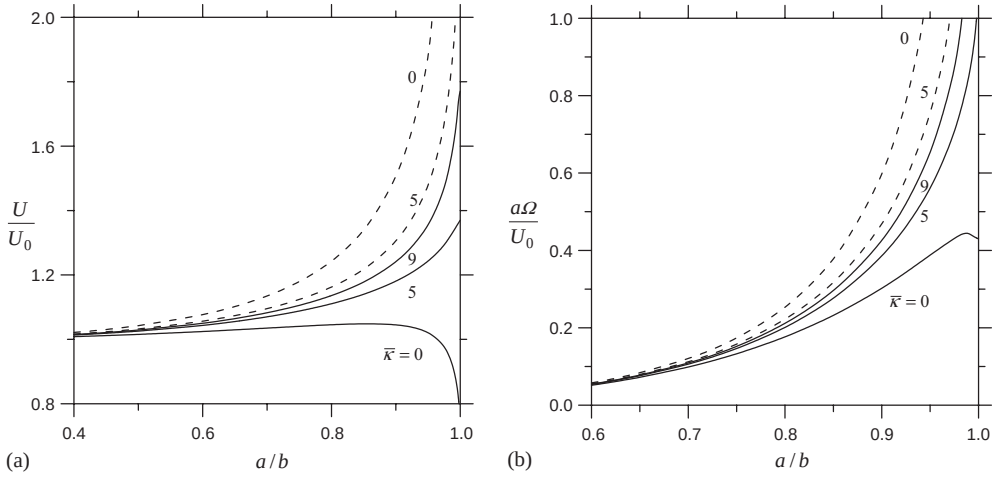

Fig. 3. Plots of the normalized velocities of a spherical vesicle with $\kappa = 10$ undergoing osmophoresis parallel to a plane wall versus the separation parameter a/b for various values of $\bar{\kappa}$: (a) translational velocity U/U_0; (b) rotational velocity $a\Omega/U_0$. The solid curves represent the case of an impermeable wall, and the dashed curves denote the case of a wall on which the far-field solute concentration gradient is imposed.

Table 4
Numerical results of the normalized osmophoretic force F^* and torque T^* on a spherical vesicle located between two parallel impermeable plane walls caused by a parallel solute concentration gradient for the case of $c = 3b$ and $\kappa = \bar{\kappa} = 0$

a/b	F^*			T^*		
	$N = M = 30$	$N = M = 36$	$N = M = 42$	$N = M = 30$	$N = M = 36$	$N = M = 42$
0.2	1.15212	1.15212	1.15212	0.00163	0.00163	0.00163
0.4	1.37226	1.37226	1.37226	0.01353	0.01353	0.01353
0.6	1.72793	1.72793	1.72793	0.06345	0.06345	0.06345
0.8	2.44265	2.44265	2.44265	0.26737	0.26737	0.26737
0.9	3.29992	3.29992	3.29992	0.64857	0.64857	0.64857
0.95	4.3397	4.3397	4.3397	1.2346	1.2346	1.2346
0.99	7.7313	7.7023	7.7023	3.4525	3.4857	3.4857
0.995	9.444	9.356	9.356	4.508	4.627	4.627
0.999	12.19	11.81	11.81	5.712	6.240	6.240

Table 5
Normalized osmophoretic velocity of a spherical vesicle along the median plane between two parallel plane walls computed from the exact boundary-collocation solution and the asymptotic method-of-reflection solution

a/b	U/U_0					
	$\kappa = \bar{\kappa} = 0$		$\kappa = 10\ \bar{\kappa} = 0$		$\kappa = 0\ \bar{\kappa} = 10$	
	Exact solution	Asymptotic solution	Exact solution	Asymptotic solution	Exact solution	Asymptotic solution
For impermeable plane walls						
0.2	1.00769	1.00768	1.00466	1.00466	1.00769	1.00768
0.4	1.05744	1.05679	1.03219	1.03158	1.05752	1.05679
0.6	1.17967	1.16731	1.08410	1.07284	1.18171	1.16731
0.8	1.41975	1.32204	1.12970	1.05479	1.44544	1.32204
0.9	1.65366	1.39811	1.11592	0.97239	1.75945	1.39811
0.95	1.8903	1.43086	1.0659	0.89872	2.1753	1.43086
0.99	2.5380	1.45290	0.8984	0.81936	3.9278	1.45290
0.995	2.763		0.833		4.690	
0.999	2.949		0.727		5.392	
For plane walls prescribed with the far-field solute concentration profile						
0.2	1.00557	1.00556	1.00784	1.00784	1.00557	1.00556
0.4	1.03967	1.03894	1.05880	1.05837	1.03959	1.03894
0.6	1.11187	1.09879	1.18650	1.17561	1.11008	1.09879
0.8	1.21302	1.12156	1.45732	1.35552	1.19382	1.12156
0.9	1.27225	1.07292	1.76466	1.46018	1.21050	1.07292
0.95	1.3081	1.02076	2.1223	1.51388	1.1851	1.02076
0.99	1.3557	0.96126	3.1040	1.55682	1.0744	0.96126
0.995	1.349		3.352		1.023	
0.999	1.283		3.400		0.920	

The converged collocation solutions for the normalized velocity U/U_0 of a spherical vesicle undergoing osmophoresis on the median plane between two parallel plane walls (with $c = b$ and $\Omega = 0$) for various values of the parameters κ, $\bar{\kappa}$, and a/b are presented in Table 5 for both cases of impermeable walls and walls prescribed with the far-field solute concentration distribution. The corresponding method-of-reflection solutions, given by Eq. (A.20) in Appendix A as a power series expansion in $\lambda\ (=a/b)$ correct to $O(\lambda^7)$, are also listed in this table for comparison. Similar to the case of migration of a spherical vesicle parallel to a single plane wall considered in the previous subsection, the approximate analytical formula of Eq. (A.20) agrees very well with the exact results as long as $\lambda \leqslant 0.6$, but can have significant errors when $\lambda \geqslant 0.8$. In general, Eq. (A.20) underestimates the osmophoretic velocity of the vesicle. A comparison between Table 5 for the case of a slit and Tables 2 and 3 for the case of a single parallel plane indicates that the assumption that the boundary effect for two walls can be obtained by simple addition of single-wall effects leads to a smaller correction to osmophoretic motion as a/b is small but can give a greater correction as a/b becomes large.

In Fig. 4, the collocation results for the normalized osmophoretic mobility U/U_0 of a spherical vesicle migrating on the median plane between two parallel plane walls are plotted as functions of a/b for several values of κ and $\bar{\kappa}$. Analogous to the corresponding motion of a vesicle parallel to a single plane wall, for a specified value of a/b, U/U_0 increases with an increase in κ and with a decrease in $\bar{\kappa}$ for the case of walls with the imposed far-field solute concentration gradient and decreases with an increase in κ and with a decrease in $\bar{\kappa}$ for the case of impermeable walls. Again, for the case of impermeable walls under the situation of $\kappa \gg 1 + \bar{\kappa}$, or for the case of walls prescribed with the far-field concentration distribution under the situation of $\kappa \ll 1 + \bar{\kappa}$, the osmophoretic mobility of the vesicle first goes through a maximum with the increase of a/b from $a/b = 0$ and then decreases monotonically, and the vesicle can even move slower than it would at $a/b = 0$. This result indicates that the effect of solutal retardation, rather than that of hydrodynamic enhancement, can be overriding when the vesicle-wall gap thickness is small. An examination of the asymptotic formula for U/U_0 in Eq. (A.20) also shows a good agreement of the trend in Fig. 4 with the analytical solution.

A careful comparison of the curves in Fig. 4 for the case of a slit with the corresponding curves in Figs. 2a and 3a for the case of a single wall reveals an interesting feature of the boundary effect on osmophoresis of a spherical vesicle. The presence of a second, identical, lateral plane wall, even at a symmetric position with respect to the vesicle against the first, does not always enhance the wall effect on the osmophoretic vesicle induced by the first plate only. This result reflects again the fact that the lateral wall can affect the osmotic driving force and the hydrodynamic force on

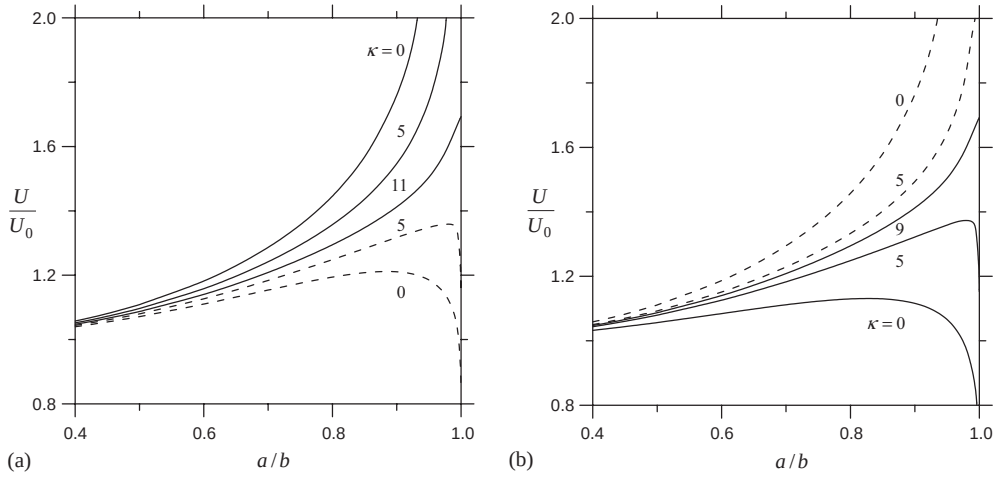

Fig. 4. Plots of the normalized osmophoretic mobility U/U_0 of a spherical vesicle migrating on the median plane between two parallel plane walls (with $c = b$) versus the separation parameter a/b: (a) for several values of κ with $\bar{\kappa} = 10$; (b) for several values of $\bar{\kappa}$ with $\kappa = 10$. The solid curves represent the case of an impermeable wall, and the dashed curves denote the case of walls prescribed with the far-field solute concentration distribution.

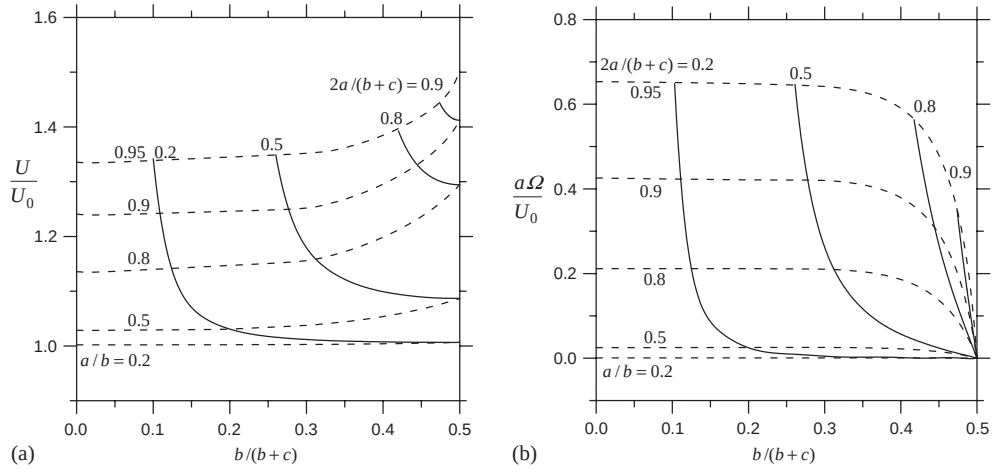

Fig. 5. Plots of the normalized velocities of a spherical vesicle undergoing osmophoresis parallel to two plane walls versus the ratio $b/(b + c)$ for the case of $\kappa = 1 + \bar{\kappa}$ with a/b and $2a/(b + c)$ as parameters: (a) translational velocity U/U_0; (b) rotational velocity $a\Omega/U_0$.

a vesicle in opposite directions. Each force is increased in its own direction as the value of a/b turns small, but to a different degree, for the case of osmophoretic motion of a vesicle in a slit relative to that for the case of migration parallel to a single plate. Thus, the net effect composed of these two opposite forces for the slit case is not necessarily to enhance that for the case of a single wall.

Fig. 5 shows the collocation results for the normalized translational velocity U/U_0 and rotational velocity $a\Omega/U_0$ of a spherical vesicle undergoing osmophoresis parallel to two plane walls at various positions between them for a general case with $\kappa = 1 + \bar{\kappa}$. The dashed curves (with $a/b =$ constant) illustrate the effect of the position of the second wall (at $z = c$) on the vesicle velocities for various values of the relative vesicle-to-first-wall spacing b/a. The solid curves (with $2a/(b + c) =$ constant) indicate the variation of the vesicle velocities as functions of the vesicle position at various values of the relative wall-to-wall spacing $(b + c)/2a$. As illustrated in Fig. 5a, the net wall effect for the given case is to increase the osmophoretic mobility U/U_0 of the vesicle. At a constant value of $2a/(b + c)$, the vesicle has a smallest translational velocity (without rotation) when it is located midway between the two walls (with $c = b$). Both the translational and rotational velocities increase as the vesicle approaches either of the walls (or the ratio $b/(b+c)$ decreases). At a specified value of a/b for the osmophoretic vesicle near a first lateral wall, the presence of a second plate is to further increase the translational velocity of the vesicle, and the degree of this enhancement increases monotonically with a decrease in the relative distance between the vesicle and the second plate (or with an increase in $b/(b + c)$). On the other hand, the rotational velocity of the vesicle is a monotonic decreasing function of $b/(b+c)$ for an otherwise unchanged situation.

On the other hand, for some cases such as the migration of a spherical vesicle with $\kappa \gg 1+\bar{\kappa}$ parallel to two impermeable plane walls or with $\kappa \ll 1+\bar{\kappa}$ parallel to two plates prescribed with the far-field solute concentration distribution, the net wall effect can decrease the osmophoretic mobility of the vesicle relative to its isolated value. At a fixed value of $2a/(b+c)$ in these cases, the normalized osmophoretic mobility of the vesicle has a relatively large value as it is located midway between the two walls, where the vesicle experiences a minimum effect of solutal retardation, and becomes relatively small when it approaches either of the walls. At a given value of a/b for the osmophoretic vesicle and the first lateral plate, the effect induced by the presence of the second plate on the vesicle mobility is not necessarily a monotonic function of its distance from the vesicle. This dependence is not graphically presented here for conciseness.

4. Conclusions

In this article, the exact numerical solutions and approximate analytical solutions for the quasisteady osmophoretic motion of a spherical vesicle parallel to two infinite plane walls at an arbitrary position between them have been obtained by using the boundary-collocation technique and the method of reflections, respectively. Both the cases of impermeable walls and of walls with the imposed far-field solute concentration gradient were examined in the limit of vanishingly small Reynolds and Peclet numbers. It has been found that the boundary effect on osmophoretic motion of a vesicle is quite complicated. The osmophoretic mobility of a vesicle near a wall is generally, but not necessarily, a monotonic increasing function of the separation parameter a/b. When the value of a/b is close to unity, the effect of a lateral wall can speed up or slow down the vesicle velocity relative to its isolated value depending on the relative values of the parameters κ and $\bar{\kappa}$ and the solutal boundary condition at the wall. This behavior reflects the competition between the hydrodynamic enhancement exerted by the neighboring wall on the vesicle migration and the possible osmophoretic retardation due to the solutal interaction between the vesicle and the lateral wall.

Notation

a	radius of the vesicle, m
A	osmophoretic mobility defined by Eq. (1b), $m^5 s^{-1}$
A_n, B_n, C_n	coefficients in Eq. (19) for the flow field, $m^{n+1}s^{-1}$, $m^{n+3}s^{-1}$, $m^{n+2}s^{-1}$
b, c	the respective distances from the vesicle center to the two plates, m
C	solute concentration field outside the vesicle, m^{-3}
C_0	value of C_∞ at the position of vesicle center, m^{-3}
C_1	solute concentration field inside the vesicle, m^{-3}
$\bar{C}$	average solute concentration inside the vesicle, m^{-3}
C_∞	prescribed solute concentration field defined by Eq. (6), m^{-3}
$\mathbf{e}_x, \mathbf{e}_y, \mathbf{e}_z$	unit vectors in rectangular coordinates
$\mathbf{e}_r, \mathbf{e}_\theta, \mathbf{e}_\phi$	unit vectors in spherical coordinates
E_∞	$=\lvert\nabla C_\infty\rvert$, m^{-4}
F^*	normalized osmophoretic force on the vesicle
G	dimensionless parameter defined right after Eq. (A.4)
L_p	hydraulic coefficient of the vesicle membrane, $m^2 s\,kg^{-1}$
r	radial spherical coordinate, m
R	the gas constant, $J\,K^{-1}$
$R_n, \bar{R}_n$	coefficients in Eqs. (10)–(12) for the solute concentration field, m^{n+2}, m^{-n+1}
T	absolute temperature, K
T^*	normalized osmophoretic torque on the vesicle
$\mathbf{U}, U$	translational velocity of the vesicle, $m\,s^{-1}$
$\mathbf{U}_0, U_0$	osmophoretic velocity of an isolated vesicle defined by Eq. (1), $m\,s^{-1}$
$\mathbf{v}$	velocity field of the fluid, $m\,s^{-1}$
x, y, z	rectangular coordinates, m

Greek letters

$\delta_n^{(1)}, \delta_n^{(2)}$,	functions of r and μ defined by Eqs. (B.1)–(B.2), m^{-n-1}, m^{-n-2},
η	viscosity of the fluid, $kg\,m^{-1}s^{-1}$
θ, ϕ	angular spherical coordinates
$\kappa, \bar{\kappa}$	dimensionless parameters defined by Eq. (2)
λ	$=a/b$
μ	$=\cos\theta$
ρ	radial cylindrical coordinate, m
$\mathbf{\Omega}, \Omega$	angular velocity of the vesicle, s^{-1}

Subscripts

p	vesicle
w	wall

Acknowledgements

This research was partly supported by the National Science Council of the Republic of China.

Appendix A. Analysis of the osmophoresis of a spherical vesicle parallel to plane walls by a method of reflections

In this appendix, we analyze the quasisteady osmophoretic motion of a spherical vesicle either parallel to an infinite flat wall ($c \to \infty$) or on the median plane

between two parallel plates ($c = b$), as shown in Fig. 1, by a method of reflections. The effect of the walls on the translational velocity $\mathbf{U}$ and angular velocity $\mathbf{\Omega}$ of the vesicle is sought in expansions of λ, which equals a/b, the ratio of the vesicle radius to the distance between the wall and the center of the vesicle.

A.1. Motion parallel to an infinite plane wall

For the problem of osmophoretic motion of a spherical vesicle parallel to an impermeable plane wall, the governing equations (3a) and (14) must be solved by satisfying the boundary conditions (4)–(6) and (15)–(17) with $c \to \infty$. The method-of-reflection solution consists of the following series, whose terms depend on increasing powers of λ:

$$C = C_0 - E_\infty x + C_p^{(1)} + C_w^{(1)} + C_p^{(2)} + C_w^{(2)} + \cdots, \quad \text{(A.1a)}$$

$$\mathbf{v} = \mathbf{v}_p^{(1)} + \mathbf{v}_w^{(1)} + \mathbf{v}_p^{(2)} + \mathbf{v}_w^{(2)} + \cdots, \quad \text{(A.1b)}$$

where subscripts w and p represent the reflections from wall and vesicle, respectively, and the superscript (i) denotes the ith reflection from that surface. In these series, all the expansion sets of the corresponding solute concentration and fluid velocity for the solution phase outside the vesicle must satisfy Eqs. (3a) and (14). The advantage of this method is that it is necessary to consider boundary conditions associated with only one surface at a time.

According to Eq. (A.1), the translational and angular velocities of the vesicle can also be expressed in the series form,

$$\mathbf{U} = U_0\mathbf{e}_x + \mathbf{U}^{(1)} + \mathbf{U}^{(2)} + \cdots, \quad \text{(A.2a)}$$

$$\mathbf{\Omega} = \mathbf{\Omega}^{(1)} + \mathbf{\Omega}^{(2)} + \cdots. \quad \text{(A.2b)}$$

In these expressions, $U_0 = AE_\infty$ is the osmophoretic velocity of an identical vesicle suspended freely in the continuous phase far from the wall given by Eq. (1); $\mathbf{U}^{(i)}$ and $\mathbf{\Omega}^{(i)}$ are related to $\nabla C_w^{(i)}$ and $\mathbf{v}_w^{(i)}$ by (Keh and Tu, 2000)

$$\mathbf{U}^{(i)} = -A[\nabla C_w^{(i)}]_0 + [\mathbf{v}_w^{(i)}]_0 + \frac{a^2}{6}[\nabla^2\mathbf{v}_w^{(i)}]_0, \quad \text{(A.3a)}$$

$$\mathbf{\Omega}^{(i)} = \frac{1}{2}[\nabla \times \mathbf{v}_w^{(i)}]_0, \quad \text{(A.3b)}$$

where the subscript 0 to variables inside brackets denotes evaluation at the position of the vesicle center.

The solution for the first reflected fields from the vesicle is

$$C_p^{(1)} = -GE_\infty a^3 r^{-2}\sin\theta\cos\phi, \quad \text{(A.4a)}$$

$$\mathbf{v}_p^{(1)} = -U_0 a^3 r^{-3}(2\sin\theta\cos\phi\,\mathbf{e}_r - \cos\theta\cos\phi\mathbf{e}_\theta + \sin\phi\,\mathbf{e}_\phi), \quad \text{(A.4b)}$$

where $G = (1 + \bar\kappa - \kappa)(2 + 2\bar\kappa + \kappa)^{-1}$. Obviously, $-1 \leqslant G \leqslant 1/2$, with the upper and lower bounds occurring at the limits $\kappa \ll 1 + \bar\kappa$ and $\kappa \gg 2(1 + \bar\kappa)$, respectively. The velocity distribution shown in Eq. (A.4b) is identical to the irrotational flow surrounding a rigid sphere moving with velocity $-2U_0\mathbf{e}_x$.

The boundary conditions for the ith reflected fields from the wall are derived from Eqs. (5), (6), (16), and (17),

$$z = -b: \quad \frac{\partial C_w^{(i)}}{\partial z} = -\frac{\partial C_p^{(i)}}{\partial z}, \quad \text{(A.5a)}$$

$$\mathbf{v}_w^{(i)} = -\mathbf{v}_p^{(i)}; \quad \text{(A.5b)}$$

$$r \to \infty, \quad z > -b: \quad C_w^{(i)} \to 0, \quad \text{(A.5c)}$$

$$\mathbf{v}_w^{(i)} \to \mathbf{0}. \quad \text{(A.5d)}$$

The solution of $C_w^{(1)}$ is obtained by applying complex Fourier transforms on x and y in Eqs. (3a) and (A.5a) and (A.5c) (taking $i = 1$), with the result

$$C_w^{(1)} = -GE_\infty a^3 x[x^2 + y^2 + (z + 2b)^2]^{-3/2}. \quad \text{(A.6a)}$$

This reflected concentration field may be interpreted as arising from the reflection of the imposed field $-E_\infty\mathbf{e}_x$ from a fictitious vesicle identical to the actual vesicle, its location being at the mirror-image position of the actual vesicle with respect to the plane $z = -b$ (i.e. at $x = 0$, $y = 0$, $z = -2b$). The solution for $\mathbf{v}_w^{(1)}$ can be found by fitting the boundary conditions (A.5b) and (A.5d) with the general solution to Eq. (14) established by Faxen (Happel & Brenner, 1983, p. 323), which results in

$$\mathbf{v}_w^{(1)} = -\frac{U_0 a^3}{2\pi}\int_{-\infty}^{\infty}\int_{-\infty}^{\infty} \mathrm{e}^{\mathrm{i}(\alpha x + \beta y) - \gamma(z+2b)} \left\{-[2\gamma(z+b)+1]\mathrm{i}\alpha\mathbf{e}_z - \left[2(z+b) - \frac{1}{\gamma}\right](\alpha^2\mathbf{e}_x + \alpha\beta\mathbf{e}_y)\right\} \mathrm{d}\alpha\,\mathrm{d}\beta, \quad \text{(A.6b)}$$

where $\gamma = (\alpha^2 + \beta^2)^{1/2}$, and $\mathrm{i} = \sqrt{-1}$.

The contributions of $C_w^{(1)}$ and $\mathbf{v}_w^{(1)}$ to the translational and angular velocities of the vesicle are determined by using Eq. (A.3),

$$\mathbf{U}_s^{(1)} = -A[\nabla C_w^{(1)}]_{r=0} = \frac{1}{8}G\lambda^3 U_0\mathbf{e}_x, \quad \text{(A.7a)}$$

$$\mathbf{U}_h^{(1)} = [\mathbf{v}_w^{(1)} + \frac{a^2}{6}\nabla^2\mathbf{v}_w^{(1)}]_{r=0} = \frac{1}{4}(\lambda^3 - \lambda^5)U_0\mathbf{e}_x, \quad \text{(A.7b)}$$

$$\mathbf{U}^{(1)} = \mathbf{U}_s^{(1)} + \mathbf{U}_h^{(1)} = \left[\frac{1}{8}(2+G)\lambda^3 - \frac{1}{4}\lambda^5\right]U_0\mathbf{e}_x, \quad \text{(A.7c)}$$

$$a\mathbf{\Omega}^{(1)} = \frac{a}{2}[\nabla \times \mathbf{v}_w^{(1)}]_{r=0} = \frac{3}{8}\lambda^4 U_0\mathbf{e}_y. \quad \text{(A.7d)}$$

Equation (A.7a) shows that the reflected solute concentration field from the impermeable wall can increase (if $G > 0$

or $\kappa < 1 + \bar{\kappa}$) or decrease (if $G < 0$ or $\kappa > 1 + \bar{\kappa}$) the translational velocity of the osmophoretic vesicle, while Eq. (A.7b) indicates that the reflected velocity field is to *increase* this velocity; the net effect of the reflected fields is expressed by Eq. (A.7c), which can enhance or retard the movement of the vesicle, depending on the combination of the values of G (or κ and $\bar{\kappa}$) and λ. When $G=0$ (or $\kappa=1+\bar{\kappa}$), the reflected concentration field makes no contribution to the osmophoretic velocity. Eq. (A.7c) indicates that the wall correction to the translational velocity of the osmophoretic vesicle is $O(\lambda^3)$, which is weaker than that obtained for the corresponding sedimentation problem, in which the leading boundary effect is $O(\lambda)$. Note that the necessary condition for the wall retardation on the osmophoretic motion to occur is $\kappa \gg 1 + \bar{\kappa}$ and a value of λ close to unity such that the relation $\lambda^5 > (1 + G/2)\lambda^3$ is warranted.

Eq. (A.7d) shows that the osmophoretic sphere rotates about an axis which is perpendicular to the direction of the applied solute gradient and parallel to the plane wall. The direction of rotation is the same as that which would occur if a rigid sphere is driven to move parallel to the plane wall by a body force. Note that the angular velocity $\boldsymbol{\Omega}^{(1)}$ in Eq. (A.7d) does not depend on the parameter G (since $\mathbf{v}_w^{(1)}$ is not a function of G). Also, the wall-induced angular velocity of the osmophoretic vesicle is $O(\lambda^4)$, which is the same in order as but different in its coefficient (3/8 versus 3/32) from that of a rigid sphere moving under a body-force field (Happel and Brenner, 1983, p. 327).

The solution for the second reflected fields from the vesicle is

$$C_p^{(2)} = -\frac{1}{8} E_\infty [G^2\lambda^3 a^3 r^{-2} \sin\theta\cos\phi + 3GH\lambda^4 a^4 r^{-3} \cos\theta\sin\theta\cos\phi + O(\lambda^5 a^5)], \tag{A.8a}$$

$$\begin{aligned}\mathbf{v}_p^{(2)} = -\frac{1}{16} U_0 [&2G\lambda^3 a^3 r^{-3}(2\sin\theta\cos\phi\,\mathbf{e}_r - \cos\theta\cos\phi\,\mathbf{e}_\theta + \sin\phi\,\mathbf{e}_\phi) \\ &- 3\left(2G\frac{B}{A} - 15\right)\lambda^4 a^2 r^{-2}\cos\theta\sin\theta\cos\phi\,\mathbf{e}_r \\ &- 6\lambda^4 a^2 r^{-2}(\cos\phi\,\mathbf{e}_\theta - \cos\theta\sin\phi\,\mathbf{e}_\phi) \\ &+ O(\lambda^4 a^4, \lambda^5 a^3)].\end{aligned} \tag{A.8b}$$

Here, $H = (2 + \bar{\kappa} - \kappa)(6 + 3\bar{\kappa} + 2\kappa)^{-1}$, $B = 5aL_pRT(6 + 3\bar{\kappa} + 2\kappa)^{-1}$.

The boundary conditions for the second reflected fields from the wall are obtained by substituting the results of $C_p^{(2)}$ and $\mathbf{v}_p^{(2)}$ into Eq. (A.5), with which Eqs. (3a) and (14) can be solved as before to yield

$$[\nabla C_w^{(2)}]_{r=0} = -\left[\frac{1}{64} G^2\lambda^6 + O(\lambda^8)\right] E_\infty \mathbf{e}_x, \tag{A.9a}$$

$$\begin{aligned}[\mathbf{v}_w^{(2)}]_{r=0} &= \left\{\frac{1}{128}\left[39 + 2\left(2 - 3\frac{B}{A}\right)G\right]\lambda^6 + O(\lambda^8)\right\} U_0\mathbf{e}_x \\ &= \left\{\frac{1}{128}\left[39 + 2\left(2 - 3\frac{B}{A}\right)G\right]\lambda^6 + O(\lambda^8)\right\} U_0\mathbf{e}_x\end{aligned} \tag{A.9b}$$

The contribution of the second reflected fields to the translational and angular velocities of the vesicle is obtained by combining Eqs. (A.3) and (A.9), which gives

$$\mathbf{U}^{(2)} = \left\{\frac{1}{128}\left[39 + 2\left(2 - 3\frac{B}{A}\right)G + 2G^2\right]\lambda^6 + O(\lambda^8)\right\} U_0\mathbf{e}_x, \tag{A.10a}$$

$$a\boldsymbol{\Omega}^{(2)} = \left\{\frac{3}{256}\left[19 + 4\left(1 - 8\frac{B}{A}G\right)\right]\lambda^7 + O(\lambda^9)\right\} U_0\mathbf{e}_y. \tag{A.10b}$$

The errors for $\mathbf{U}^{(2)}$ and $a\boldsymbol{\Omega}^{(2)}$ are $O(\lambda^8)$ and $O(\lambda^9)$, respectively, because the $O(\lambda^7)$ terms in the expansions of $\nabla C_w^{(2)}$ and $\mathbf{v}_w^{(2)}$ vanish at the position of the vesicle center.

Obviously, $\mathbf{U}^{(3)}$ and $a\boldsymbol{\Omega}^{(3)}$ will be $O(\lambda^9)$ and $O(\lambda^{10})$, respectively. With the substitution of Eqs. (A.7c), (A.7d) and (A.10) into Eq. (A.2), the vesicle velocities can be expressed as $\mathbf{U} = U\mathbf{e}_x$ and $\boldsymbol{\Omega} = \Omega\mathbf{e}_y$ with

$$U = U_0\left\{1 + \frac{1}{8}(2 + G)\lambda^3 - \frac{1}{4}\lambda^5 + \frac{1}{128}\left[39 + 2\left(2 - 3\frac{B}{A}\right)G + 2G^2\right]\lambda^6 + O(\lambda^8)\right\}, \tag{A.11a}$$

$$a\Omega = U_0\left\{\frac{3}{8}\lambda^4 + \frac{3}{256}\left[19 + 4\left(1 - 8\frac{B}{A}\right)G\right]\lambda^7 + O(\lambda^9)\right\}. \tag{A.11b}$$

The vesicle migrates along the imposed concentration gradient at a rate that can increase or decrease as the vesicle approaches the wall. Owing to the neglect of inertial effects, the wall does not deflect the direction of osmophoresis.

For the case that a linear concentration profile is prescribed on the plane wall which is consistent with the far-field solute distribution, namely, the boundary condition (5) is replaced by Eq. (7), the series expansions (A.1) and (A.2), the solution of $C_p^{(1)}$ and $\mathbf{v}_p^{(1)}$ in Eq. (A.4), and the boundary conditions for $C_w^{(i)}$ and $\mathbf{v}_w^{(i)}$ in Eqs. (A.5b)–(A.5d) are still valid, while Eq. (A.5a) becomes

$$z = -b: \quad C_w^{(i)} = -C_p^{(i)}. \tag{A.12}$$

With this change, it can be shown that the results of the following reflected fields and of the vesicle velocities are

also obtained from Eqs. (A.6)–(A.11) by replacing G by $-G$. Thus, contrary to the effect of an impermeable plane wall, the reflected concentration field from a parallel wall with the imposed far-field concentration gradient reduces the translational velocity of the vesicle if $G > 0$ or $\kappa < 1 + \bar{\kappa}$ and enhances this velocity if $G < 0$ or $\kappa > 1 + \bar{\kappa}$. When $G = 0$ or $\kappa = 1 + \bar{\kappa}$, the two types of plane wall will produce the same effects (with no contribution from the reflected solute concentration field) on the osmophoretic motion of the vesicle. Under the condition that $\kappa \ll 1 + \bar{\kappa}$ and the value of λ is sufficiently large such that $\lambda^5 > (1 - G/2)\lambda^3$, the net effect of a lateral plane wall prescribed with the far-field solute concentration distribution can retard the osmophoretic migration of a vesicle.

A.2. Motion on the median plane between two parallel flat walls

For the problem of osmophoretic motion of a spherical vesicle on the median plane between two impermeable parallel plates, the boundary conditions corresponding to governing equations (3a) and (14) are given by Eqs. (4)–(6) and (15)–(17) with $c = b$. But, the angular velocity $\mathbf{\Omega}$ of the vesicle vanishes now because of the symmetry. With $\lambda = a/b \ll 1$, the series expansions of the solute concentration, fluid velocity, and vesicle velocity given by Eqs. (A.1), (A.4), and (A.2a) remain valid here. From Eqs. (5), (6), (16), and (17), the boundary conditions for $C_w^{(i)}$ and $\mathbf{v}_w^{(i)}$ are found to be

$$|z| = b: \quad \frac{\partial C_w^{(i)}}{\partial z} = -\frac{\partial C_p^{(i)}}{\partial z}, \tag{A.13a}$$

$$\mathbf{v}_w^{(i)} = -\mathbf{v}_p^{(i)}; \tag{A.13b}$$

$$r \to \infty, \quad |z| \leqslant b: \quad C_w^{(i)} \to 0, \tag{A.13c}$$

$$\mathbf{v}_w^{(i)} \to 0. \tag{A.13d}$$

The first wall-reflected fields can be solved by the same method as used for a single lateral plate in the previous subsection, with the results

$$C_w^{(1)} = \frac{GE_\infty a^3}{2\pi} \int_{-\infty}^{\infty}\int_{-\infty}^{\infty} \frac{\mathrm{i}\alpha}{\gamma}\, \mathrm{e}^{\mathrm{i}(\alpha x+\beta y)-\gamma b} \frac{\cosh(\gamma z)}{\sinh(\gamma b)}\, \mathrm{d}\alpha\, \mathrm{d}\beta, \tag{A.14a}$$

$$\mathbf{v}_w^{(1)} = -\frac{U_0 a^3}{\pi} \int_{-\infty}^{\infty}\int_{-\infty}^{\infty} \frac{1}{\sinh(2\gamma b) - 2\gamma b}\, \mathrm{e}^{\mathrm{i}(\alpha x+\beta y)} \{[\sinh(\gamma z) - \gamma z\cosh(\gamma z) + g\sinh(\gamma z)]\mathrm{i}\alpha\mathbf{e}_z + [z\sinh(\gamma z) - \frac{g}{\gamma}\cosh(\gamma z)](\alpha^2 \mathbf{e}_x + \alpha\beta\mathbf{e}_y)\}\, \mathrm{d}\alpha\, \mathrm{d}\beta, \tag{A.14b}$$

where $\gamma = (\alpha^2 + \beta^2)^{1/2}$ and $g = \gamma b - \mathrm{e}^{-\gamma b}\sinh(\gamma b)$. The contributions of $C_w^{(1)}$ and $\mathbf{v}_w^{(1)}$ to the vesicle velocity are determined using Eq. (A.3a), which lead to a result similar to Eqs. (A.7a)–(A.7c),

$$\mathbf{U}_s^{(1)} = d_1 G\lambda^3 U_0 \mathbf{e}_x, \tag{A.15a}$$

$$\mathbf{U}_h^{(1)} = (d_2\lambda^3 - d_3\lambda^5)U_0\mathbf{e}_x, \tag{A.15b}$$

$$\mathbf{U}^{(1)} = \mathbf{U}_s^{(1)} + U_h^{(1)} = [(d_2 + d_1 G)\lambda^3 - d_3\lambda^5]U_0\mathbf{e}_x, \tag{A.15c}$$

where

$$d_1 = \int_0^\infty \frac{\rho^2}{\mathrm{e}^{2\rho} - 1}\, \mathrm{d}\rho = 0.300514, \tag{A.16a}$$

$$d_2 = \int_0^\infty \frac{\rho^2(\rho - \mathrm{e}^{-\rho}\sinh\rho)}{\sinh(2\rho) - 2\rho}\, \mathrm{d}\rho = 0.835912, \tag{A.16b}$$

$$d_3 = \frac{1}{3}\int_0^\infty \frac{\rho^4}{\sinh(2\rho) - 2\rho}\, \mathrm{d}\rho = 0.676648. \tag{A.16c}$$

Analogous to the previous case, the results of the second reflections can be obtained as

$$C_p^{(2)} = -E_\infty[d_1 G^2\lambda^3 a^3 r^{-2}\sin\theta\cos\phi + O(\lambda^5 a^5)], \tag{A.17a}$$

$$\mathbf{v}_p^{(2)} = U_0[-d_1 G\lambda^3 a^3 r^{-3}(2\sin\theta\cos\phi\mathbf{e}_r - \cos\theta\cos\phi\mathbf{e}_\theta + \sin\phi\mathbf{e}_\phi) + O(\lambda^5 a^3)], \tag{A.17b}$$

$$[\nabla C_w^{(2)}]_{r=0} = -[d_1^2 G^2\lambda^6 + O(\lambda^8)]E_\infty\mathbf{e}_x, \tag{A.18a}$$

$$[\mathbf{v}_w^{(2)}]_{r=0} = [d_1 d_2 G\lambda^6 + O(\lambda^8)]U_0\mathbf{e}_x, \tag{A.18b}$$

and

$$\mathbf{U}^{(2)} = [(d_1 d_2 G + d_1^2 G^2)\lambda^6 + O(\lambda^8)]U_0\mathbf{e}_x. \tag{A.19}$$

Note that the $\lambda^4 a^2$ and $\lambda^4 a^4$ terms in the expressions for $C_p^{(2)}$ and $\mathbf{v}_p^{(2)}$ vanish. With the combination of Eqs. (A.2a), (A.15c), and (A.19), the vesicle velocity can be expressed as $\mathbf{U} = U\mathbf{e}_x$ with

$$U = U_0[1 + (d_2 + d_1 G)\lambda^3 - d_3\lambda^5 + (d_1 d_2 G + d_1^2 G^2)\lambda^6 + O(\lambda^8)]. \tag{A.20}$$

For the case that the vesicle is undergoing osmophoresis on the median plane between two parallel plates on which a linear concentration profile consistent with the far-field solute distribution is imposed, the boundary condition given by Eq. (5) should be replaced by Eq. (7). In this case, Eqs. (A.1), (A.2), (A.4) and (A.13b)–(A.13d) are still applicable, while Eq. (A.13a) becomes

$$|z| = b: \quad C_w^{(i)} = -C_p^{(i)}. \tag{A.21}$$

With this change, it can be shown that the results of the reflected fields and of the vesicle velocity are also obtained from Eq. (A.14)–(A.20) by replacing G and d_1 by $-G$ and $\bar{d}_1$, respectively, where

$$\bar{d}_1 = \int_0^\infty \frac{\rho^2}{e^{2\rho}+1}\,d\rho = 0.225386. \tag{A.22}$$

Comparing Eq. (A.20) for the slit case with Eq. (A.11a) for the case of a single parallel plane, one can find that the wall effects on the osmophoretic velocity of a vesicle in the two cases are qualitatively similar. However, the assumption that the result of the boundary effect for two walls can be obtained by simple addition of the single-wall effects generally gives a smaller correction to the osmophoretic velocity, while for the corresponding sedimentation problem this approximation overestimates the wall correction.

Appendix B. Definitions of some functions in Section 2

The functions $\delta_n^{(1)}$ and $\delta_n^{(2)}$ in Eqs. (12), (13), and (20) are defined by

$$\delta_n^{(1)}(r,\mu) = r^{-n-1}P_n^1(\mu) - (-n)^m \int_0^\infty \gamma^{1-m}\frac{J_1(\gamma\rho)}{\sinh\tau} [c^2 V_{n+m}(c)(\sinh\sigma)^{1-m}(\cosh\sigma)^m - b^2 V_{n+m}(-b)(\sinh\omega)^{1-m}(\cosh\omega)^m]\,d\gamma, \tag{B.1}$$

$$\delta_n^{(2)}(r,\mu) = -(n+1)r^{-n-2}P_n^1(\mu) - (-n)^m \int_0^\infty \frac{\gamma^{2-m}}{\sinh\tau} \{J_1'(\gamma\rho)(1-\mu^2)^{1/2} \times [c^2 V_{n+m}(c)(\sinh\sigma)^{1-m}(\cosh\sigma)^m - b^2 V_{n+m}(-b)(\sinh\omega)^{1-m}(\cosh\omega)^m] + J_1(\gamma\rho)\mu[c^2 V_{n+m}(c)(\cosh\sigma)^{1-m}(\sinh\sigma)^m - b^2 V_{n+m}(-b)(\cosh\omega)^{1-m}(\sinh\omega)^m]\}\,d\gamma, \tag{B.2}$$

where

$$V_n(z_i) = \frac{(2/\pi)^{1/2}}{z_i^{n+1}} \sum_{q=0}^{[n/2]} \frac{(\gamma|z_i|)^{n-q-(1/2)}}{(-2)^q q!(n-2q-1)!} K_{n-q-(3/2)}(\gamma|z_i|), \tag{B.3}$$

$$\sigma = \gamma(z+b), \quad \omega = \gamma(z-c), \quad \tau = \gamma(b+c), \tag{B.4a,b,c}$$

J_1 is the Bessel function of the first kind of order one and the prime on it denotes differentiation with respect to its argument, K_ν is the modified Bessel function of the second kind of order ν, and the square bracket $[\nu]$ denotes the largest integer which is less than or equal to ν. In Eqs. (B.1) and (B.2), $m=1$ if Eq. (5) is used for the boundary condition of the solute concentration filed at the plane walls and $m=0$ if Eq. (7) is used.

References

Anderson, J. L. (1983). Movement of a semipermeable vesicle through an osmotic gradient. *Physics of Fluids*, *26*, 2871–2879.

Anderson, J. L. (1986). Transport mechanisms of biological colloids. *Annals of the New York Academy of Sciences (Biochemical Engineering IV)*, *469*, 166–177.

Berg, H. C., & Turner, L. (1990). Chemotaxis of bacteria in glass capillary arrays. *Biophysical Journal*, *58*, 919–930.

Ganatos, P., Weinbaum, S., & Pfeffer, R. (1980). A strong interaction theory for the creeping motion of a sphere between plane parallel boundaries. Part 2. Parallel motion. *Journal of Fluid Mechanics*, *99*, 755–783.

Gordeon, L. G. M. (1981). Osmophoresis. *Journal of Physical Chemistry*, *85*, 1753–1755.

Happel, J., & Brenner, H. (1983). *Low Reynolds number hydrodynamics*. Dordrecht, The Netherlands: Nijhoff.

Keh, H. J., & Tu, H. J. (2000). Osmophoresis in a dilute suspension of spherical vesicles. *International Journal of Multiphase Flow*, *26*, 125–145.

Keh, H. J., & Yang, F. R. (1993a). Boundary effects on osmophoresis: Motion of a vesicle normal to a plane wall. *Chemical Engineering Science*, *48*, 609–616.

Keh, H. J., & Yang, F. R. (1993b). Boundary effects on osmophoresis: Motion of a vesicle in an arbitrary direction with respect to a plane wall. *Chemical Engineering Science*, *48*, 3555–3563.

Nardi, J., Bruinsma, R., & Sackmann, E. (1999). Vesicles as osmotic motors. *Physical Review Letters*, *82*, 5168–5171.

O'Brien, V. (1968). Form factors for deformed spheroids in Stokes flow. *A.I.Ch.E. Journal*, *14*, 870–875.